Antibody Recognition of Cancer Cells via Glycan Surface Engineering

Mathieu Szponarski[a] and Karl Gademann*[a]

Stimulation of the body's immune system toward tumor cells is now well recognized as a promising strategy in cancer therapy. Just behind cell therapy and monoclonal antibodies, small molecule-based strategies are receiving growing attention as alternatives to direct immune response against tumor cells. However, the development of small-molecule approaches to modulate the balance between stimulatory immune factors and suppressive factors in a targeted way remains a challenge. Here, we report the cell surface functionalization of LS174T cancer cells with an abiotic hapten to recruit antibodies to the cell surface. Metabolic glycoengineering followed by covalent reaction with the hapten results in antibody recognition of the target cells. Microscopy and flow cytometry studies provide compelling evidence that metabolic glycoengineering and small molecule stimulators can be combined to direct antibody recognition.

Introduction

The development and use of synthetic systems to control the human immune response (synthetic immunology), has become an important research area in medicine.[1–4] From small molecules to recombinant proteins and the engineering of autologous immune cells, synthetic immunology spans many areas of research from the cellular to the molecular level. Checkpoint inhibitors[5–8] and more recently chimeric antigen receptor (CAR) T-cell therapies[3,9–11] are two key hallmarks of synthetic immunology that translated into major advances in the clinic. At a molecular level, the potential of chemical compounds to boost the immune response toward tumors has gained increased attention and is now well recognized.[3,12–16] In contrast to antibodies or cell therapies, small molecules have the advantage of being orally bioavailable, crossing cell membranes, and being relatively inexpensive to produce. The development of cancer-specific small molecule tags that modulate T-cell co-stimulation or boost immune recognition therefore seems desirable. In this context, the concept of antibody-recruiting small molecules (ARMs), consisting of bifunctional molecules containing an antibody-binding terminus (*e.g.*, dinitrophenyl, biotin, galactosyl-(1-3)-galactose, L-rhamnose) and a target-binding terminus (binding a cancer specific receptor) has been explored.[17–28] One of the advantages of the ARM approach is that the target-binding terminus can be readily selected from known binders of the target receptor sparing any major investigations from that side. The major hurdle to overcome however, is to find a suitable position to tether the antibody-binding terminus without impeding the binding affinity of the ARM and structure-activity relationship studies thus represent a downside of this approach. While this process can be alleviated by computational design, if available,[24,25] often a number of derivatives need to be prepared and tested.[25]

Metabolic glycoengineering, based on the conversion of abiotic biosynthetic precursors to unnatural surface glycoconjugates has become one of the methods of choice for cell surface functionalization. Pioneered by Bertozzi and co-workers,[29] glycoengineering with azido-sugars coupled with strain-promoted azide-alkyne cycloaddition (SPAAC)[30–32] quickly found diverse applications.[33] On the methods side, advances in the understanding of metabolic pathways combined with sophisticated molecular design led to significantly improved systems.[34] For example, Cheng and co-workers demonstrated that metabolic glycoengineering could be rendered selective toward cancer cells overexpressing histone deacetylase and cathepsin-L by protecting the azido-sugar with an acetylated lysin motif. Applying this method, selective incorporation of azide moieties on the surface of tumor cells both *in vitro* and *in vivo* could be achieved.[35] In the context of our research program on surface engineering with new-to-nature catalyst systems,[36] antibiotics,[37,38] proteins,[39] to biohybrid microswimmers,[40] we became interested in antibody recruiting to cell surfaces.

We reasoned that the functionalization of the cell surface with an antibody recruiting small molecule by metabolic glycoengineering would represent an attractive alternative to ARMs.[41] The metabolic glycoengineering approach could combine both the versatility and the selectivity needed for further potential therapeutic application. Few previous approaches have focused on antibody recruiting via metabolic glycoengineering via various immunostimulants,[42] polymeric systems,[43] immunogenic sialic acid precursors,[44] or H_2O_2-responsive glycan metabolic precursors.[45] Wang, Wang, and co-authors reported on a folate-receptor selective glycoengineering strategy with subsequent rhamnose labelling,[46] which

[a] *M. Szponarski, K. Gademann*
Department of Chemistry
University of Zurich, 8057 Zurich (Switzerland)
E-mail: karl.gademann@uzh.ch

Supporting information for this article is available on the WWW under https://doi.org/10.1002/cbic.202200125

was used for both fluorescent imaging and antibody labelling. Selective glycoengineering was also achieved by galactosidase-mediated activation of suitable precursors.[47] All these approaches offer several advantages and limitations, which have been recently reviewed.[41,48]

In this study, we report the surface functionalization of live LS174T cells with a DNP hapten by metabolic glycoengineering. The resulting functionalized cells are able to recruit anti-DNP antibodies to their surface as supported by confocal microscopy and flow cytometry analyses. This study reports on one of the smallest immunostimulant modifications so far.

Results

Synthesis of the clickable hapten

We designed the clickable immunostimulant **1** for our studies. Hapten **1** bears a dinitrophenyl (DNP) moiety as the antibody-recruiting motif at one end, a polyethylene glycol chain as a spacer and a dibenzocyclooctene at the other end for the SPAAC chemistry. The clickable DNP hapten was synthesized in four steps starting from commercially available 1-chloro-2,4-dinitrobenzene (**2**) (Scheme 1). Nucleophilic aromatic substitution on **2** with 2,2′(ethylenedioxy)diethylamine in refluxing ethanol quantitatively yielded derivative **3**. Reaction of **3** with succinic anhydride in MeCN at room temperature gave access to carboxylic acid **4** with good yields. Compound **4** was then coupled to dibenzocyclooctyne-amine *via* activation with *N*-hydroxysuccinimide and DCC in DMF. The desired clickable hapten **1** was then purified by reversed-phase preparative HPLC.

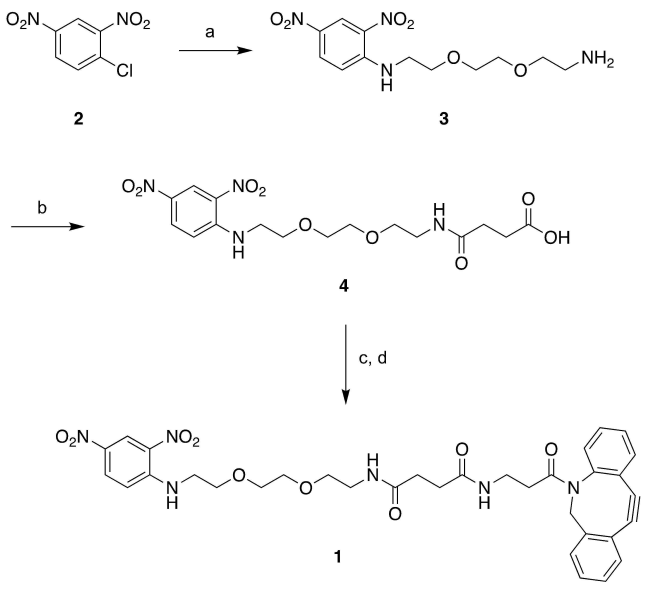

Scheme 1. Synthesis of the clickable DNP hapten **1**. Reagents and conditions: a) 2,2′- (ethylenedioxy)diethylamine, EtOH, reflux, 2.5 h, quant.; b) succinic anhydride, MeCN, rt, 3 h, 82%; c) *N*-hydroxysuccinimide, DCC, DMF, 0 °C to rt, 20 h; d) dibenzocyclooctyne-amine, Et_3N, DMF, rt, 24 h, 51% (over two steps).

Microscopy studies

With the clickable DNP hapten **1** in hand, we then moved on to the metabolic glycoengineering. For our proof of concept study, we chose LS174T colorectal cancer cells, a cell-line that has been shown to overexpress both HDAC and CTSL required for the ATTACK strategy developed by Cheng and co-workers.[35] Before installing the DNP hapten, preliminary experiments were carried out confirming that Ac_4ManNAz (**5**) could be successfully incorporated on the surface of LS174T cells and leveraged to click a Cy5 Dye (Supporting Figure SF1). Estimation of the amount on azide moieties under the assumption of complete click reaction with the dye resulted in $230 \pm 54 \times 10^6$ azide units per LS174T cell (SI and Supporting Figure SF2). Next, we repeated the metabolic glycoengineering process but this time for the installation of the DNP hapten **1**, to probe its ability to recruit anti DNP antibodies to the cell surface. Cells were seeded in chambered coverslips and allowed to attach for 16 h. Cells were then incubated with Ac_4ManNAz (**5**) (50 μM) for 72 h, washed with phosphate-buffered saline (PBS) and incubated with DNP hapten **1** (50 μM) in DMEM for 16 h. Blocking was carried out with PBS containing 2% of bovine serum albumin (BSA), cells were incubated with Alexa 488-conjugated rabbit anti-dinitrophenyl IgG (20 $\mu g\,mL^{-1}$) for 60 min and then washed with PBS (Figure 1). Cells were fixed with 4% paraformaldehyde, stained with DAPI and samples were mounted on a microscopy slide.

In addition to the sample treated as described above, a series of control samples was also prepared. All samples were then imaged by confocal laser scanning microscopy (Figure 2). As expected, for cells incubated with the Alexa 488-conjugated rabbit anti-dinitrophenyl IgG only (Figure 2 sample B), no fluorescence signal could be detected on the Alexa 488 channel compared to the non-treated control (Figure 2 sample A). This first observation confirmed that no unspecific binding of the anti-DNP labelled antibody could be detected. For sample C, consisting of LS174T cells incubated with the DNP hapten **1** followed by incubation with the labelled anti-DNP antibody, no signal on the Alexa 488 channel was detected either. This demonstrated that the "clickable" DNP hapten **1** was not interacting with the cells in any way without prior metabolic engineering with Ac_4ManNAz (**5**). The absence of signal on the Alexa 488 channel in sample D, consisting of LS174T cells incubated with Ac_4ManNAz (**5**) for 72 h followed by incubation with the labelled anti-DNP antibody, confirmed that the azide moieties installed on the surface by metabolic glycoengineering were not able to recruit the anti-DNP antibody. In contrast, a clear signal could be detected on the Alexa 488 channel of sample E consisting of cells treated with Ac_4ManNAz **(5)** for 72 h, then with DNP hapten **1** and finally with Alexa 488-conjugated rabbit anti-dinitrophenyl IgG. Together, these results demonstrate that only cells functionalized with the DNP

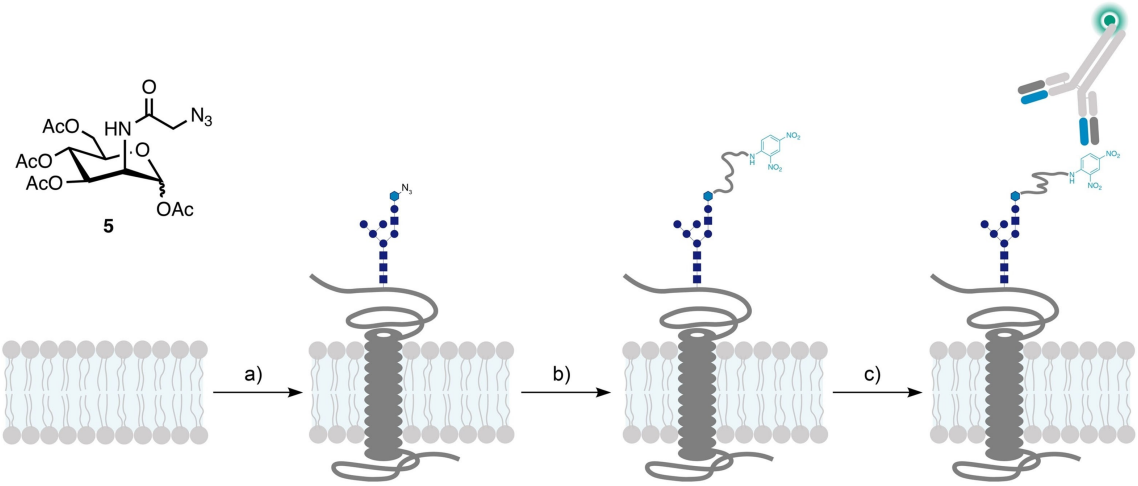

Figure 1. Functionalization of the cell surface with hapten **1** for recruitment of an antibody to the cell surface. Conditions: a) Ac_4ManNAz (**5**) (50 μM), b) DNP hapten **1** (50 μM); c) Alexa 488-conjugated anti-DNP IgG (20 μg mL^{-1}).

hapten could successfully recruit the anti-DNP antibody to their surface.

Flow cytometry studies

To corroborate the previous microscopy results and further characterize the recruitment of the anti-DNP antibodies by the clickable DNP hapten, we next performed flow cytometry experiments. LS174T cells were seeded in 24 well-plates and incubated with Ac_4ManNAz (**5**) at a concentration of 50 μM for 72 h. To remove any unmetabolized Ac_4ManNAz, cells were washed and then incubated with increased concentrations of the DNP hapten **1** for 19 h. Removal of unreacted **1** was ensured by washing of the cells. Cells were then lifted by treatment with trypsin, incubated with Alexa 488-conjugated rabbit anti-dinitrophenyl IgG (10 μg mL^{-1}) on ice for 30 min, pelleted, washed, and resuspended for flow cytometry analysis of the Alexa 488 signal.

As depicted in Figure 3a, only a very small difference in Alexa 488 median fluorescence intensity (MFI) between the untreated control sample and the sample corresponding to an absence of incubation with the DNP hapten (0 μM) was detected. This observation first confirmed the conclusion drawn from the microscopy experiments: cells only treated with Ac_4ManNAz (**5**) did not recruit the anti-DNP antibody nor did the click chemistry alone lead to antibody recruitment. Most importantly, the Alexa 488 MFI increased with the incubation concentration of the DNP hapten **1**. This observation confirmed that increased concentration of **1** translated to an increased amount of anti-DNP antibody on the cell surface. The reason for this observation is that under the assumption of constant azide concentration, the overall reaction rate is proportional to the amount of DNP hapten **1** employed. If the reaction is stopped and evaluated at a certain time point before full conversion, higher concentrations of **1** translate into higher concentrations of hapten on the surface. Taken together, these experiments further demonstrate that recruitment of this antibody to the cell surface is directed by the DNP hapten. As depicted in Figure 3b, histogram plots of the Alexa 488 intensity showed a relatively narrow population distribution of the treated cells demonstrating the homogeneity of the functionalization process and the subsequent antibody recruitment.

Cytotoxicity of the DNP hapten

Having demonstrated that hapten **1** can recruit antibodies to the cell surface, we then evaluated its cytotoxicity. As depicted in Figure 4, no appreciable cytotoxicity was detected below a concentration of 10 μM after 48 h of incubation. Interestingly, higher concentrations did show a cytotoxic effect. In our case however, the previous flow cytometry experiments showed that the anti-DNP antibody could be recruited *via* functionalization of the cells with **1** at concentrations within its non-cytotoxic range.

Discussion

In summary, we demonstrated that covalent cell surface engineering with abiotic dinitrophenyl derivatives can be leveraged for antibody recognition. We provided evidence that metabolic glycoengineering followed by click chemistry can be used to functionalize live cells with dinitrophenyl haptens. The functionalized cells were able to recruit anti-DNP antibodies to their surface as confirmed by confocal microscopy and flow cytometry experiments. This study complements different approaches based on other haptens or labelling methods.[46] Compared to other approaches such as ARMs or polymeric systems,[21–26,41–54] this approach presents the flexibility of a two-step glycoengineering/labelling approach. Furthermore, the

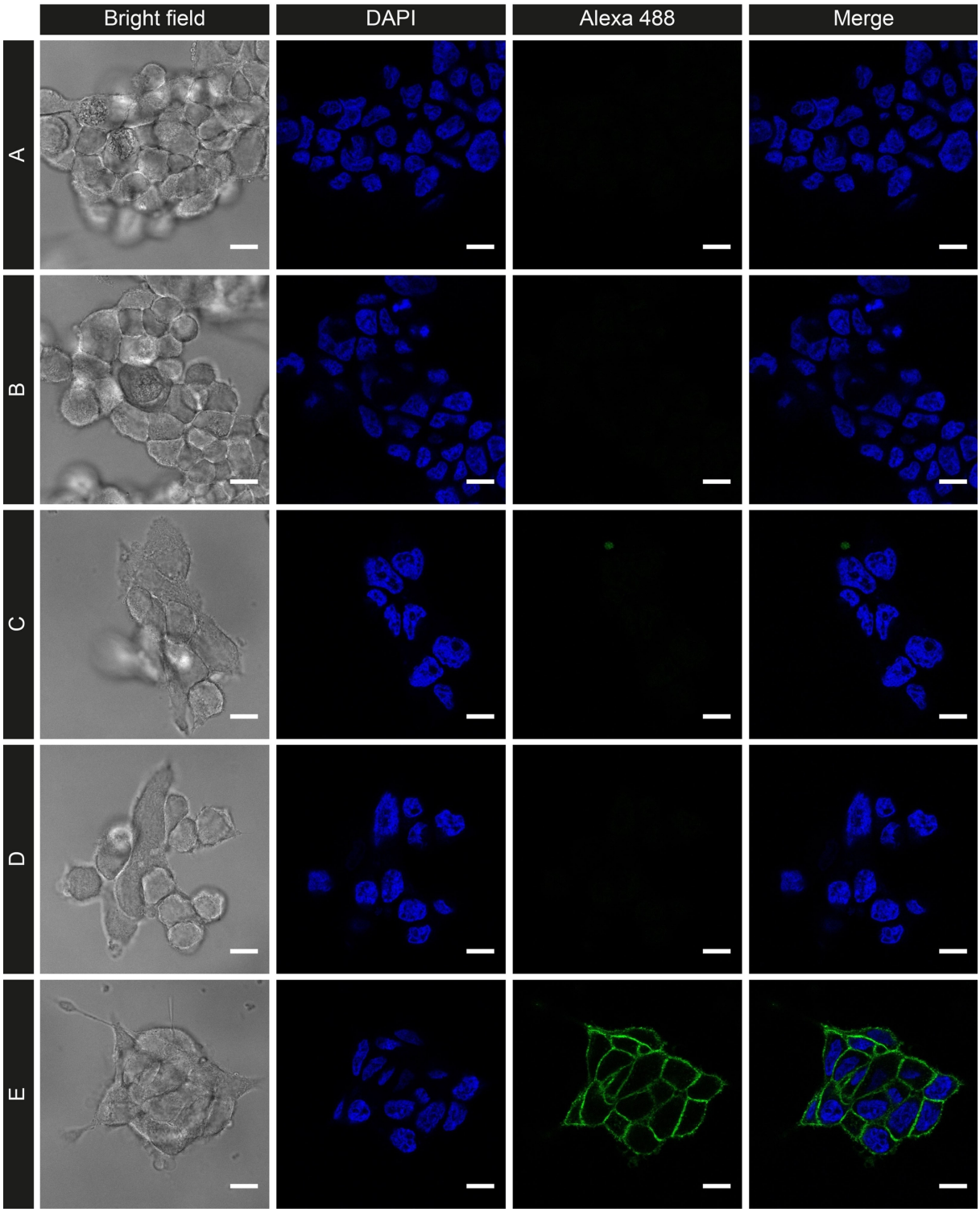

Figure 2. Cell surface functionalization with DNP hapten **1** followed by immunolabeling. CLSM images. Scale bar: 10 μm. Sample A: not treated; sample B: Alexa 488-conjugated anti-DNP IgG (20 μg mL^{-1}); sample C: DNP hapten **1** (50 μM), Alexa 488-conjugated anti-DNP IgG (20 μg mL^{-1}); sample D: Ac_4ManNAz (**5**) (50 μM), Alexa 488-conjugated anti-DNP IgG (20 μg mL^{-1}); sample E: Ac_4ManNAz (**5**) (50 μM), DNP hapten **1** (50 μM), Alexa 488-conjugated anti-DNP IgG (20 μg mL^{-1}).

general approach described here could be leveraged by selective metabolic glycoengineering strategies targeting specifically cancer cells.[34,35,46,47] Challenges to this approach potentially include limited concentration of the hapten on the cell surface, slow or mismatched kinetics of glycoengineering and labelling vs. internalization or degradation, and reduced

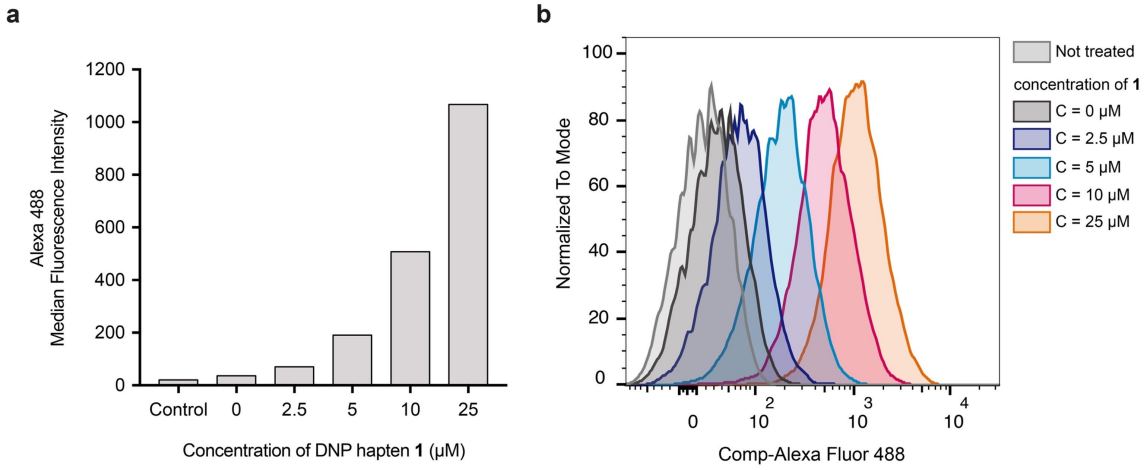

Figure 3. Flow cytometry analysis of the influence of the DNP hapten concentration on the recruitment of the anti-DNP antibody. Conditions: Ac_4ManNAz (**5**) (50 μM) 72 h, then DNP hapten **1** (0–25 μM), 72 h, then Alexa 488-conjugated anti-DNP IgG (10 μg mL^{-1}), 60 min. **a** Alexa 488 MFI increases with incubation concentration of DNP hapten **1**; **b** Histogram plot, intensity of Alexa 488 cell population increases with incubation concentration of DNP hapten **1**.

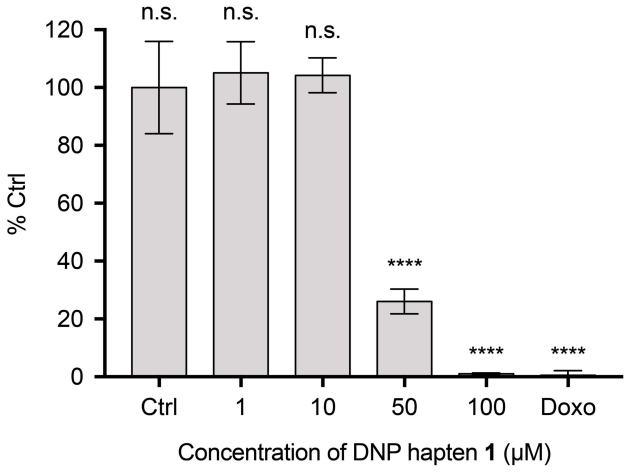

Figure 4. Evaluation of the cytotoxicity of the hapten **1** on LS174T cells. The cytotoxicity was determined after 48 h of incubation by evaluation of dehydrogenase activity with CCK-8. Doxorubicin (Doxo) was used as control.

efficacy of covalent linkage of the hapten to tumor cells. Further studies will demonstrate the scope and limitations of this and complementary approaches. In this context, one could envision the translation of an intracellular cancer specific property into a cell surface signature recognized by endogenous antibodies. Given the applicability and the versatility of this approach, our goal is to further develop this method to trigger and modulate immune response.

Experimental Section

Purchased chemicals were used without further purification (unless otherwise stated). DBCO-Cy5.5 was purchased from Jena bioscience (CLK-1046-5). Ac_4ManNAz was purchased from Jena bioscience (CLK-1084-5). Alexa 488-conjugated rabbit anti-dinitrophenyl IgG was purchased from Thermo Fisher Scientific (A-11097). Prolong Diamond Antifade Mounted was purchased from Thermo Fisher Scientific (P35965). DMEM was purchased from Sigma-Aldrich (D6046). PBS was purchased from Gibco. FBS, Pen/Strep and Trypsin-EDTA were purchased from Gibco. BSA was purchased from Sigma-Aldrich (A9647). DAPI was purchased from Roche (10 236 276 001). CCK-8 was purchased from Sigma-Aldrich (96992). TC-treated culture flasks were purchased from Corning. TC-treated chambered coverslips were purchased from Eppendorf.

Cell culture

LS174T Human colorectal cancer cells (ACC-759) were purchased from the Deutsche Sammlung von Mikroorganismen und Zellkulturen (DSMZ) and stored in liquid nitrogen. Cells were cultured in DMEM containing 10% FBS and 100 units mL^{-1} Penicillin G and 100 μg mL^{-1} Streptomycin at 37 °C in 5% CO_2 humidified air in 75 cm^3 TC-treated culture flasks.

Synthesis

***N*-(2-(2-(2-Aminoethoxy)ethoxy)ethyl)-2,4-dinitroaniline (3)**: 1-Chloro-2,4-dinitrobenzene (**2**) (742 mg, 3.66 mmol, 1.0 eq.), and 2,2′-(ethylenedioxy)diethylamine (2.70 mL, 18.5 mmol, 5.1 eq.) were added in EtOH (18.0 mL). The mixture was heated to reflux for 2.5 h and went from deep yellow to orange. The reaction mixture was then concentrated under reduced pressure, diluted with H_2O (20 mL), brine (20 mL), an aq. sat. solution of $NaHCO_3$ (20 mL) and the product was extracted with CH_2Cl_2 (3×15 mL). The organic layer was then washed with an aq. NaCl solution (50% saturated, 2× 25 mL), dried over $MgSO_4$ and filtered. Volatiles were removed under reduced pressure to yield the desired aniline **3** (1.15 g, 3.66 mmol, quant.) as an orange oil.

FTIR: ν = 3359, 2879, 1619, 1586, 1523, 1501, 1424, 1334, 1305, 1132, 919, 832 cm^{-1}. **^{1}H NMR** (400 MHz, $CDCl_3$) δ = 9.07 (s, 1H), 8.78 (s, 1H), 8.22 (d, *J* = 8.0 Hz, 1H), 6.96–6.89 (m, 1H), 3.82 (t, *J* = 5.0 Hz, 2H), 3.75–3.56 (m, 6H), 3.53 (t, *J* = 4.9 Hz, 2H), 2.88 (t, *J* = 5.3 Hz, 2H), 2.48 (s, 2H). **^{13}C NMR** (101 MHz, $CDCl_3$) δ = 148.5, 136.1, 130.3, 124.3, 114.2, 72.9, 70.8, 70.3, 68.6, 43.3, 41.6. **HRMS (ESI)**: Calc. for $C_{12}H_{19}O_6N_4$ $[M+H]^+$: 315.12991; found: $[M+H]^+$ 315.12988.

4-((2-(2-(2-((2,4-Dinitrophenyl)amino)ethoxy)ethoxy)ethyl)amino)-4-oxobutanoic acid (4): Compound **3** (511 mg, 1.60 mmol, 1.0 eq.) was dissolved in MeCN (7.0 mL). A solution of succinic anhydride (196 mg, 1.96 mmol, 1.2 eq.) in MeCN (4.0 mL) was added dropwise and the reaction was vigorously stirred at rt for 3 h. MeCN was blown away by nitrogen stream and the crude yellow residue was purified by flash column chromatography on silica gel (CH_2Cl_2/MeOH, 98:2 to 90:10) to give the desired carboxylic acid **4** (554 mg, 1.34 mmol, 82% yield) as an orange oil.

R_f = 0.5 (CH_2Cl_2/MeOH, 96:4). **FTIR**: ν = 3356, 2923, 1728, 1618, 1586, 1523, 1424, 1333, 1303, 1265, 1132, 1092, 919, 832, 743, 507 cm^{-1}. **^{1}H NMR** (400 MHz, $CDCl_3$) δ = 9.08 (d, *J* = 2.6 Hz, 1H), 8.85 (t, *J* = 4.9 Hz, 1H), 8.25 (dd, *J* = 9.5, 2.7 Hz, 1H), 6.94 (d, *J* = 9.5 Hz, 1H), 6.62 (t, *J* = 5.5 Hz, 1H), 3.84 (t, *J* = 5.2 Hz, 2H), 3.73-3.68 (m, 2H), 3.67-3.59 (m, 4H), 3.57 (t, *J* = 5.1 Hz, 2H), 3.46 (q, *J* = 5.2 Hz, 2H), 2.69-2.59 (m, 2H), 2.54 (t, *J* = 6.6 Hz, 2H). **^{13}C NMR** (101 MHz, $CDCl_3$) δ = 175.9, 173.0, 148.5, 136.2, 130.5, 124.4, 114.3, 70.8, 70.3, 69.9, 68.3, 43.2, 39.8, 30.7, 30.1. **HRMS (ESI)**: Calc. for $C_{16}H_{23}O_9N_4$ $[M+H]^+$: 415.14595; found: $[M+Na]^+$ 415.14615.

Clickable DNP hapten (1): Carboxylic acid **4** (104 mg, 251 μmol, 1.0 eq.) was dissolved in anhydrous DMF (1.9 mL) at rt. *N*-hydroxysuccinimide (29.0 mg, 252 μmol, 1.0 eq.) and DCC (67 mg, 325 μmol, 1.3 eq.) were added at 0 °C. The reaction mixture was then stirred at rt for 20 h. The precipitate was filtered off, the filtrate was concentrated by nitrogen stream and the residue was washed with cold Et_2O. This crude product was directly used for the next step.

Dibenzocyclootyne-amine (20.0 mg, 72.4 μmol, 1.0 eq.) was dissolved in anhydrous DMF (1.5 mL), Et_3N (30.8 μL, 217 μmol, 3.0 eq.) was added at rt and the reaction mixture was stirred for 10 min at rt. The crude succinimide ester previously obtained (37 mg, 72.4 μmol, 1.0 eq.) was then added at rt and the reaction was stirred at rt for 24 h. The solvent was blown away by nitrogen stream and the sample dried under reduced pressure. The crude product was dissolved in MeCN, filtered on a SPE column, MeCN was removed under reduced pressure and the crude residue was purified by reversed-phase preparative HPLC.

Purification was conducted on a Gemini®-NX 5 μm C18 110 Å LC column (250×21.2 mm) eluting with 0.1% formic acid in H_2O (solvent A) and 0.1% formic acid in MeCN (solvent B), applying the following gradient: 0.00–8.00 min 40% B, 8.00–48.00 min 40% to 100% B, 48.00–65.00 min 100% B, at a flow rate of 20.0 mL min^{-1} at 25 °C, with detection and fraction collection at 254 nm. MeCN was evaporated under reduced pressure and the compound was lyophilized from H_2O to give **1** (25.0 mg, 37.2 mmol, 51% yield) as a yellow foam.

FTIR: ν = 3347, 1650, 1620, 1588, 1524, 1428, 1335, 1305, 1135, 755 cm^{-1}. **^{1}H NMR** (400 MHz, $CDCl_3$) δ = 9.12 (s, 1H), 8.83 (s, 1H), 8.26 (dt, *J* = 9.5, 1.8 Hz, 1H), 7.67 (d, *J* = 7.5 Hz, 1H), 7.41–7.27 (m, 7H), 6.92 (d, *J* = 9.5 Hz, 1H), 6.44 (br s, 1H), 6.20 (br s, 1H), 5.13 (d, *J* = 13.9 Hz, 1H), 3.82 (t, *J* = 5.2 Hz, 2H), 3.73-3.66 (m, 3H), 3.65–3.56 (m, 4H), 3.54 (t, *J* = 5.2 Hz, 2H), 3.43 (q, *J* = 5.4 Hz, 2H), 3.38–3.29 (m, 1H), 3.25–3.15 (m, 1H), 2.51–2.38 (m, 3H), 2.37–2.28 (m, 2H), 2.00–1.90 (m, 1H). **HRMS (ESI)**: Calc. for $C_{34}H_{36}O_9N_6$ $[M+H]^+$: 673.26165; found: $[M+H]^+$ 673.26141.

Cell surface functionalization with DBCO-Cy5

LS174T Cells were seeded on gelatin-coated coverslips, placed in 6-well plates in DMEM containing 10% FBS and 1% pen-strep (total volume of 2.0 mL per well) at a cell density of $4{\cdot}10^4$ cells per well and allowed to attach for 16 h. Ac_4ManNAz (**5**) (50 μM, from a 50 mM stock solution in DMSO) was added to the cells (control samples received the same volume of DMSO). Cells were then incubated at 37 °C, 5% CO_2, 90% humidity for 72 h. After washing of the samples with PBS (3×1 mL per well) cells were incubated with DBCO-Cy5 (60 μM from a 50 mM stock solution in DMSO) in PBS containing 1% FBS (2.0 mL) for 1 h in an orbital shaker at rt. Samples were then washed with PBS (3×1 mL) to remove the excess of the DBCO-Cy5 probe, DMEM (1 mL) spiked with 20% of a 4% solution of paraformaldehyde was added to the cells for 2 min and aspirated. Samples were then fixed by treatment with a 4% solution of paraformaldehyde (1 mL) for 15 min, followed by gentle rinsing with PBS (1×1 mL). Staining of the cell nuclei was performed by incubation of the fixed cells with DAPI (2.0 μg mL^{-1} in PBS) for 15 min in the dark followed by gentle washing with PBS (1×1 mL). The coverslips were then removed from the 6-well plate, mounted with Prolong Diamond Antifade Mountant and air dried for 24 h before imaging.

Microscopy studies of the surface functionalization with hapten (1)

LS174T Cells were seeded in TC-treated 8-well chambered coverslips in DMEM containing 10% FBS and 1% pen-strep (total volume of 500 μL per well) at a density of $1{\cdot}10^4$ cells per well and allowed to attach for 16 h. Ac_4ManNAz (**5**) (50 μM from a 50 mM stock solution in DMSO) was added to the cells (control samples received the same volume of DMSO). Cells were then incubated at 37 °C, 5% CO_2, 90% humidity for 72 h. After washing with DMEM (3×500 μL) cells were then incubated with the clickable hapten **1** (50 μM, from 50 mM stock solution in DMSO) in DMEM (total volume of 500 μL) in the incubator overnight. Cells were washed with buffer A (1X PBS, 2% w/v BSA, 3×500 μL) and Alexa 488-conjugated rabbit anti-dinitrophenyl IgG (20 μg mL^{-1} in buffer A) was added to the cells (total volume of 300 μL). Cultures were protected from light and incubated at 37 °C in the CO_2 incubator for 60 min. The cells were then washed with PBS (2×500 μL), and fixed by the addition of a 4% solution of paraformaldehyde (400 μL) for 15 min, followed by gentle rinsing with PBS (2×500 μL). Staining of the cell nuclei was performed by incubation of the fixed cells with DAPI (2.0 μg mL^{-1} in PBS) for 15 min in the dark followed by gentle washing with PBS (1×500 μL). The chambered coverslip was then disassembled, mounted with Prolong Diamond Antifade Mountant and air dried for 24 h before imaging. Samples where then imaged by CLSM.

Flow cytometry studies of the surface functionalization with hapten (1)

LS174T Cells were seeded in a 24-well plate in DMEM containing 10% FBS and 1% pen-strep (total volume of 400 μL) at $6{\cdot}10^4$ cells per well and allowed to attach for 16–20 h. Ac_4ManNAz (**5**) (50 μM, from a 50 mM stock solution in DMSO) was added to the cells (control samples received the same volume of DMSO). Cells were then incubated at 37 °C, 5% CO_2, 90% humidity for 72 h. After washing with DMEM (2×500 μL) cells were then incubated with the clickable hapten **1** (2.5–25 μM, from a 50 mM stock solution in DMSO) in DMEM (total volume of 400 μL) in the incubator overnight. All samples were then washed with PBS (2×500 μL). Cells from each well were harvested by treatment with 0.25% Trypsin-EDTA (150 μL) for 5 min, diluted to a total volume of 500 μL with buffer A (1X PBS, 2% w/v BSA) and transferred to Eppendorf tubes. One sample was used to determine the cell density. Cells were then pelleted (1000 RCF for 5 min) resuspended in buffer A ($5{\cdot}10^5$ cells mL^{-1}) and Alexa 488-conjugated rabbit anti-dinitrophenyl IgG (10 μg mL^{-1}) was added. Eppendorf tubes were incubated on ice for 30 min and then diluted to 1 mL with buffer A. The cells were pelleted (1000 RCF for 5 min), washed with buffer A,

pelleted again, and resuspended in buffer A at a cell density of $1 \cdot 10^6$ cells mL^{-1} for flow cytometry analysis. Sample were placed on ice and analyzed on a BD LSR Fortessa SORP (BD Biosciences). A 488 nm laser was used for the excitation of Alexa Fluor 488 and a FITC (530/30) filter for the detection of the emitted fluorescence signal (peak area).

Cytotoxicity evaluation

Cells were seeded in a 96-well plate in DMEM containing 10% FBS and 1% pen-strep (total volume of 100 μL) at a cell density of 4 000–5 000 cells per well and allowed to attach for 24 h. The medium was then removed and cells were incubated with the desired compounds at different concentrations (from a 1000X stock solution in DMSO) at 37 °C, 5% CO_2, 90% humidity for 48 or 72 h depending on the compounds. The medium was removed, cells were incubated with 10% CCK-8 (100 μL total volume) for 60 to 120 min in the CO_2 incubator, and the absorbance at 450 nm was then measured. Absorbance at 650 nm was also measured and the value was subtracted as the background (indication of any precipitation or aggregation). Values of the wells with cells incubated with DMSO only were set as control, and values of the wells without cells were set as blank.

Statistical analyses

Prism 7 was used for data analysis and representation. Statistical analysis was performed by one-way analysis of variance (ANOVA) with post hoc Tukey test (for multiple comparison) and P values < 0.05 were considered statistically significant. The results were deemed significant at $0.01 < *P \leq 0.05$, very significant at $0.001 < **P \leq 0.01$, extremely significant at $0.0001 < ***P \leq 0.001$ and extremely significant at $****P \leq 0.0001$

Supporting information

Supporting figures, imaging conditions, image processing, and statistical analyses are reported in the supplementary information.

Acknowledgements

We acknowledge the Center for Microscopy and Image Analysis (ZMB) and the Flow Cytometry Facility of the University of Zurich for training and maintenance of the instruments. Dr. Katja Zerbe and Miriam Gwerder are kindly acknowledged for initial support with the tissue culture. We acknowledge the Swiss National Science Foundation as part of the NCCR Molecular Systems Engineering, the University of Basel, and the University of Zürich for funding. Open access funding provided by the University of Zurich.

Conflict of Interest

The authors declare no conflict of interest.

Data Availability Statement

All data are included in the manuscript and the supplementary information.

Keywords: antibody · bioorganic chemistry · cancer · chemical biology · glycoengineering

[1] F. P. Polack, S. J. Thomas, N. Kitchin, J. Absalon, A. Gurtman, S. Lockhart, J. L. Perez, G. Pérez Marc, E. D. Moreira, C. Zerbini, R. Bailey, K. A. Swanson, S. Roychoudhury, K. Koury, P. Li, W. V. Kalina, D. Cooper, R. W. Frenck, L. L. Hammitt, Ö. Türeci, H. Nell, A. Schaefer, S. Ünal, D. B. Tresnan, S. Mather, P. R. Dormitzer, U. Şahin, K. U. Jansen, W. C. Gruber, *N. Engl. J. Med.* **2020**, *383*, 2603–2615.
[2] C. H. June, M. Sadelain, *N. Engl. J. Med.* **2018**, *379*, 64–73.
[3] J. L. Adams, J. Smothers, R. Srinivasan, A. Hoos, *Nat. Rev. Drug Discovery* **2015**, *14*, 603–621.
[4] D. A. Spiegel, *Nat. Chem. Biol.* **2010**, *6*, 871–872.
[5] D. M. Pardoll, *Nat. Rev. Cancer* **2012**, *12*, 252–264.
[6] A. M. Lesokhin, M. K. Callahan, M. A. Postow, J. D. Wolchok, *Sci. Transl. Med.* **2015**, *7*, 280sr1.
[7] P. Sharma, J. P. Allison, *Science* **2015**, *348*, 56–61.
[8] W. Zou, J. D. Wolchok, L. Chen, *Sci. Transl. Med.* **2016**, *8*, 328rv4.
[9] M. L. Davila, I. Riviere, X. Wang, S. Bartido, J. Park, K. Curran, S. S. Chung, J. Stefanski, O. Borquez-Ojeda, M. Olszewska, J. Qu, T. Wasielewska, Q. He, M. Fink, H. Shinglot, M. Youssif, M. Satter, Y. Wang, J. Hosey, H. Quintanilla, E. Halton, Y. Bernal, D. C. G. Bouhassira, M. E. Arcila, M. Gonen, G. J. Roboz, P. Maslak, D. Douer, M. G. Frattini, S. Giralt, M. Sadelain, R. Brentjens, *Sci. Transl. Med.* **2014**, *6*, 224ra25.
[10] S. Srivastava, S. R. Riddell, *Trends Immunol.* **2015**, *36*, 494–502.
[11] C. H. June, R. S. O'Connor, O. U. Kawalekar, S. Ghassemi, M. C. Milone, *Science* **2018**, *359*, 1361–1365.
[12] R. J. Mancini, L. Stutts, K. A. Ryu, J. K. Tom, A. P. Esser-Kahn, *ACS Chem. Biol.* **2014**, *9*, 1075–1085.
[13] H. Weinmann, *ChemMedChem* **2016**, *11*, 450–466.
[14] D. Dhanak, J. P. Edwards, A. Nguyen, P. J. Tummino, *Cell Chem. Biol.* **2017**, *24*, 1148–1160.
[15] P. L. Toogood, *Bioorg. Med. Chem. Lett.* **2018**, *28*, 319–329.
[16] B. R. Huck, L. Kötzner, K. Urbahns, *Angew. Chem. Int. Ed.* **2018**, *57*, 4412–4428; *Angew. Chem.* **2018**, *130*, 4499–4516.
[17] M. K. O'Reilly, B. E. Collins, S. Han, L. Liao, C. Rillahan, P. I. Kitov, D. R. Bundle, J. C. Paulson, *J. Am. Chem. Soc.* **2008**, *130*, 7736–7745.
[18] L. Cui, P. I. Kitov, G. C. Completo, J. C. Paulson, D. R. Bundle, *Bioconjugate Chem.* **2011**, *22*, 546–550.
[19] Y. Lu, P. S. Low, *Cancer Immunol. Immunother.* **2002**, *51*, 153–162.
[20] Y. Lu, E. Sega, P. S. Low, *Int. J. Cancer* **2005**, *116*, 710–719.
[21] Y. Lu, F. You, I. Vlahov, E. Westrick, M. Fan, P. S. Low, C. P. Leamon, *Mol. Pharm.* **2007**, *4*, 695–706.
[22] R. P. Murelli, A. X. Zhang, J. Michel, W. L. Jorgensen, D. A. Spiegel, *J. Am. Chem. Soc.* **2009**, *131*, 17090–17092.
[23] A. X. Zhang, R. P. Murelli, C. Barinka, J. Michel, A. Cocleaza, W. L. Jorgensen, J. Lubkowski, D. A. Spiegel, *J. Am. Chem. Soc.* **2010**, *132*, 12711–12716.
[24] C. E. Jakobsche, P. J. McEnaney, A. X. Zhang, D. A. Spiegel, *ACS Chem. Biol.* **2012**, *7*, 316–321.
[25] A. F. Rullo, K. J. Fitzgerald, V. Muthusamy, M. Liu, C. Yuan, M. Huang, M. Kim, A. E. Cho, D. A. Spiegel, *Angew. Chem. Int. Ed.* **2016**, *55*, 3642.
[26] M. A. Gray, R. N. Tao, S. M. Deporter, D. A. Spiegel, B. R. McNaughton, *ChemBioChem* **2016**, *17*, 155–158.
[27] R. M. Owen, C. B. Carlson, J. Xu, P. Mowery, E. Fasella, L. L. Kiessling, *ChemBioChem* **2007**, *8*, 68–82.
[28] C. B. Calson, P. Mowery, R. M. Owen, E. C. Dykhuizen, L. L. Kiessling, *ACS Chem. Biol.* **2007**, *2*, 119–127.
[29] L. K. Mahal, K. J. Yarema, C. R. Bertozzi, *Science* **1997**, *276*, 1125–1128.
[30] V. V. Rostovtsev, L. G. Green, V. V. Fokin, K. B. Sharpless, *Angew. Chem. Int. Ed.* **2002**, *41*, 2596–2599; *Angew. Chem.* **2002**, *114*, 2708–2711.
[31] N. J. Agard, J. M. Baskin, J. A. Prescher, A. Lo, C. R. Bertozzi, *ACS Chem. Biol.* **2006**, *1*, 644–648.
[32] J. M. Baskin, J. A. Prescher, S. T. Laughlin, N. J. Agard, P. V. Chang, I. A. Miller, A. Lo, J. A. Codelli, C. R. Bertozzi, *Proc. Natl. Acad. Sci. USA* **2007**, *104*, 16793–16797.

[33] a) B. A. H. Smith, C. R. Bertozzi, *Nat. Rev. Drug Discovery* **2021**, *20*, 217–244.
[34] H. Wang, D. J. Mooney, *Nat. Chem.* **2020**, *12*, 1102–1114.
[35] H. Wang, R. Wang, K. Cai, H. He, Y. Liu, J. Yen, Z. Wang, M. Xu, Y. Sun, X. Zhou, Q. Yin, L. Tang, I. T. Dobrucki, L. W. Dobrucki, E. J. Chaney, S. A. Boppart, T. M. Fan, S. Lezmi, X. Chen, L. Yin, J. Cheng, *Nat. Chem. Biol.* **2017**, *13*, 415–424.
[36] M. Szponarski, F. Schwizer, T. R. Ward, K. Gademann, *Commun. Chem.* **2018**, *1*, 84.
[37] I. P. Kerschgens, K. Gademann, *ChemBioChem* **2018**, *19*, 439–443.
[38] I. S. Shchelik, S. Sieber, K. Gademann, *Chem. Eur. J.* **2020**, *26*, 16644–16648.
[39] J. V. D. Molino, R. Carpine, K. Gademann, S. Mayfield, S. Sieber, *Algal Res.* **2022**, *61*, 102570.
[40] I. S. Shchelik, J. V. D. Molino, K. Gademann, *Acta Biomater.* **2021**, *136*, 99–110.
[41] S. Achilli, N. Berthet, O. Renaudet, *RSC Chem. Biol.* **2021**, *2*, 713–724-.
[42] A. Mongis, F. Piller, V. Piller, *Bioconjugate Chem.* **2017**, *28*, 1151–1165.
[43] A. Uvyn, R. De Coen, O. De Wever, K. Deswarte, B. N. Lambrecht, B. G. De Geest, *Chem. Commun.* **2019**, *55*, 10952–10955.
[44] B. Lin, X. Wu, H. Zhao, Y. Tian, J. Han, J. Liu, S. Han, *Chem. Sci.* **2016**, *7*, 3737–3741.
[45] S. H. Park, H. Jung, H. Lee, T. M. Kim, J. W. Cho, W. D. Jang, J. Y. Hyun, I. Shin, *Chem. Commun.* **2020**, *56*, 10650–10653.
[46] S. Li, B. Yu, J. Wang, Y. Zheng, H. Zhang, M. J. Walker, Z. Yuan, H. Zhu, J. Zhang, P. G. Wang, B. Wang, *ACS Chem. Biol.* **2018**, *13*, 1686–1694.
[47] Y. Li, L. Gong, H. Hong, H. Lin, D. Li, J. Shi, Z. Zhou, Z. Wu, *Chem. Commun.* **2022**, *58*, 2568–2571.
[48] L. Rösner, C. P. Konken, D. A. Depke, A. Rentmeister, M. Schäfers, *Curr. Opin. Chem. Biol.* **2022**, *68*, 102144.
[49] S. Abed, R. Turner, N. Serniuck, V. Tat, S. Naiel, A. Hayat, O. Mekhael, M. Vierhout, K. Ask, A. F. Rullo, *Biochem. Pharmacol.* **2021**, *190*, 114577.
[50] E. Kapcan, B. Lake, Z. Yang, A. Zhang, M. S. Miller, A. F. Rullo, *Biochemistry* **2021**, *60*, 1447–1458.
[51] S. M. Rathmann, A. R. Genady, N. Janzen, V. Anipindi, S. Czorny, A. F. Rullo, S. Sadeghi, J. F. Valliant, *Mol. Pharm.* **2021**, *18*, 2647–2656.
[52] K. Bezverbnaya, D. Moogk, D. Cummings, C. L. Baker, C. Aarts, G. Denisova, M. Sun, J. D. McNicol, R. C. Turner, A. F. Rullo, S. R. Foley, J. L. Bramson, *Cytotherapy* **2021**, *23*, 820–832.
[53] A. Uvyn, R. De Coen, M. Gruijs, C. W. Tuk, J. De Vrieze, M. van Egmond, B. G. De Geest, *Angew. Chem.* **2019**, *131*, 13122–13127.
[54] R. De Coen, L. Nuhn, C. Perera, M. Arista-Romero, M. D. P. Risseeuw, A. Freyn, R. Nachbagauer, L. Albertazzi, S. Van Calenbergh, D. A. Spiegel, B. R. Peterson, B. G. De Geest, *Biomacromolecules* **2020**, *21*, 793–802.

Manuscript received: March 2, 2022
Revised manuscript received: May 25, 2022
Accepted manuscript online: May 30, 2022
Version of record online: June 20, 2022